HOKKAIDO UNIVERSITY

Title	Fabrication of mixed α/β-SiAlON powders via salt-assisted combustion synthesis
Author(s)	Niu, Jing; Harada, Kazuto; Suzuki, Shota et al.
Citation	Journal of Alloys and Compounds, 604, 260-265 https://doi.org/10.1016/j.jallcom.2014.03.145
Issue Date	2014-08-15
Doc URL	https://hdl.handle.net/2115/56796
Type	journal article
File Information	JAC604 260-265.pdf

Hokkaido University Collection of Scholarly and Academic Papers : HUSCAP

Fabrication of mixed α/β-SiAlON powders via salt-assisted combustion synthesis

Jing Niu[1], Kazuto Harada[2], Shota Suzuki[1], Isao Nakatsugawa[2], Noriyuki Okinaka[1], Tomohiro Akiyama[1#]

[1]Center for Advanced Research of Energy and Materials, Hokkaido University, Kita 13 Nishi 8, Kitaku, Sapporo 060-8628, Japan.

[2]Combustion Synthesis Co. Ltd., Numazu, Shizuoka 410-0801, Japan.

[#]Corresponding author: Tel: +81 11 706 6842; Fax: +81 11 726 0731

E-mail address: takiyama@eng.hokudai.ac.jp

Abstract

High-quality Y- and Ca-α/β-SiAlON and α-SiAlON ceramics were synthesized via salt-assisted combustion synthesis from Si, Al, and metal oxide (Y_2O_3 and CaO) with the addition of NaCl and $MgCl_2$ under a nitrogen pressure of 1 MPa. NaCl and $MgCl_2$ were employed as they act as excellent diluents that effectively absorb the reaction heat through melting and evaporation. We found that the type of metal chlorides employed significantly affected the α/β ratio and the morphology of the product, with the use of NaCl affording high α/β ratios and equiaxed morphologies, while the use of $MgCl_2$ resulting in low α/β ratios and elongated grains. The results of this work suggest that high-purity α/β-SiAlON composite products of intended α/β ratios can be successfully fabricated by controlling the initial metal chloride content.

Keywords: SiAlON; Gas-solid reactions; Salt-assisted; Phase composition; Microstructure.

Introduction

SiAlON ceramics are widely regarded as promising structural candidate materials for high-temperature engineering applications owing to their exceptional mechanical, thermal, and chemical properties. The structure of SiAlON is based on Si_3N_4, with Si^{4+} and N^{3-} being partially replaced by Al^{3+} and O^{2-}, respectively. The ceramic typically features two types of structures: (i) α, which is of the form $M_x^{v}Si_{12-(m+n)}Al_{m+n}O_nN_{16-n}$ ($x = m/v$; v is the valence of the metal, M; M represents metals like Li, Mg, Ca, Y, and rare earth metals); and (ii) β, which is of the form $Si_{6-z}Al_zO_zN_{8-z}$, where z denotes the number of Si–N bonds substituted by the Al–O bonds ($0 < z \leq 4.2$) [1-3].

α-SiAlON has a higher Vickers hardness, and greater oxidation and erosion resistance, but lower strength and toughness than β-SiAlON. These features are considered to be associated with their microstructures, with α-SiAlON generally exhibiting equiaxed grains while β-SiAlON exhibits elongated grains. Mixed α/β-SiAlON ceramics have been extensively studied, because such materials combine the toughness of β-SiAlON and the wear resistance of α-SiAlON, providing superior mechanical properties in comparison to those of pure α-SiAlON and composites of α-SiAlON and polytypes [4-6].

Typically, α/β-SiAlON composites or pure α-SiAlON have been prepared by hot-press (HP) [6], pressure-less sintering [7], reaction sintering [8], and carbothermal reduction and nitridation (CRN) [9]. Most of these methods, however, involve the use of expensive raw materials such as high-purity Si_3N_4 and AlN, which are sintered at temperatures of 1700–1800 °C for several hours in

a nitrogen atmosphere. The application of these approaches is limited because of their requirement of expensive raw materials or complicated equipment and processes. To this end, combustion synthesis (CS) is a proven effective energy- and time-saving process for the synthesis of SiAlONs [10-14]. It has multiple advantages over the above-mentioned methods, such as the requirement of simple equipment, short reaction times, and high-purity products. However, the CS of SiAlONs with Si, Al, SiO_2, or other metal oxides under N_2 at a specific applied pressure usually gives a low product yield owing to the existence of unreacted Si, caused by the melting and coalescence of silicon particles at the combustion front. To decrease the combustion temperature as well as to reduce the overall heat released from nitridation of Al and Si, it is necessary to add a large amount of Si_3N_4 and AlN instead of Si and Al [15,16]. In addition, NH_4Cl or NH_4F additives are also required to be added to the starting materials in order to achieve complete nitridation [13,17].

In our previous studies, single-phase β-SiAlON powders were successfully synthesized by adding a small amount of metal chlorides to the reaction mixture. The added chlorides effectively absorbed some of the reaction heat as the latent heat of phase transformation, thereby promoting complete nitridation of Si [18,19]. Therefore, the focus of the present work was to synthesize mixed α/β-SiAlON and α-SiAlON ceramics with the addition of NaCl or $MgCl_2$. The effect of salts additives on the phase compositions and microstructures of the products was also investigated. The merits of selecting NaCl and $MgCl_2$ as the salts candidates in this study are expected to be the following; (1) They are inert to the initial reactants (Si, Al, and CaO/Y_2O_3). (2) They are cost-efficient and abundant salts. (3) Their melting point (around 800 °C) and boiling point

(approximately 1420 °C) are just in the temperature ranges corresponding to the two-stage exothermic reaction including nitridation of Al and Si. For this reason, the excessive reaction enthalpy that released from the nitridation of Al and Si during the processes for combustion synthesis of SiAlON can be reduced by the melting and vaporization of the salts.

2. Experimental procedure

Si (purity >99.9 %, 12 μm), Al (purity >99.9 %, 14 μm), $CaCO_3$ (purity >99.9 %), and Y_2O_3 (purity >99.9 %) powders were used as starting materials in this study. NaCl (purity >99.9 %) and $MgCl_2$ (purity >99.9 %) were used as the diluents at varying amounts. According to the general chemical formula of $M_x^vSi_{12-(m+n)}Al_{m+n}O_nN_{16-n}$ for α-SiAlON, two different compositions of α/β-SiAlON of the chemical formulae; $Y_{0.2}Si_{11.1}Al_{0.9}O_{0.3}N_{15.7}$ (m = 0.6, n = 0.3) and $Ca_{0.3}Si_{11.1}Al_{0.9}O_{0.3}N_{15.7}$ (m = 0.6, n = 0.3) were fabricated, as described by the α-SiAlON phase diagram [20,21]. α-SiAlON ceramics of the compositions of $Y_{0.4}Si_{10.2}Al_{1.8}O_{0.6}N_{15.4}$ (m = 1.2, n = 0.6) and $Ca_{0.5}Si_{10.5}Al_{1.5}O_{0.5}N_{15.5}$ (m = 1, n = 0.5) were also prepared for analysis. The syntheses of Ca-α/β-SiAlON and Ca-α-SiAlON were carried out using $CaCO_3$ and CaO (produced upon calcination of $CaCO_3$ at 1000 °C).

The mixtures were mechanically activated using a planetary ball mill (Gokin Planetaring Inc., Japan) at a ball-to-sample mass ratio of 10:1. The activated powders were then charged into a porous carbon crucible, and placed in a combustion chamber. The chamber was filled with N_2 (purity: 99.999 %) up to a pressure of 1 MPa after evacuation. A tungsten–rhenium thermocouple protected by a layer of BN was inserted into the center of the powders to record the combustion temperature profiles. The combustion reaction was triggered by passing an electric current (60 A, 10 s) through a carbon foil to ignite the Al powder (ignition agent) that was placed on top of the mixture. A detailed description of the planetary milling and equipment setup for CS is provided in a previous report [11].

Phase composition of the products were analyzed using X-ray diffraction (XRD, Miniflex, Rigaku, Japan) with CuKα radiation (λ = 1.54056 nm). The microstructures were observed using a scanning electron microscope (FE-SEM, JSM-7400F, JEOL, Japan). The amounts of α- and β-SiAlON present were estimated by comparing the intensities of the two strongest XRD peaks of the two phases, which are the (210) peaks for both α- and β-SiAlON [22].

3. Results and discussion

Fig. 1 displays the XRD patterns of combustion synthesized Y-α/β-SiAlON obtained with the addition of different amount of NaCl (mass %). The intensity of the Si peaks gradually decreased as the amount of NaCl added increased. When 12 mass % NaCl was added, only α- and β-SiAlON were detected, which indicated the complete nitridation of Si. Similar experiments were carried out with varying amounts of $MgCl_2$, as the diluent. An optimal 18 mass% $MgCl_2$ was required to achieve complete nitridation of the Si particles and obtain products consisting of both the α- and β-SiAlON crystalline phases, as shown in Fig. 2. Furthermore, the amount of α-SiAlON obtained in the product when using $MgCl_2$ was lower than that obtained using NaCl. This indicated that NaCl was more efficient at promoting the formation of α-phase SiAlON. This result is consistent with results of a previous work, which reported that α-phase Si_3N_4 content increased upon addition of NaCl for the combustion synthesis of α/β-Si_3N_4 [23].

The qualitative estimation of the relative amounts of α- and β-SiAlON in the obtained samples was performed using the relative intensities of the (210) reflections, as seen in the X-ray diffraction patterns [22] for both α-SiAlON and β-SiAlON. The relative weight fractions of the α-phase SiAlON, obtained using optimal amount of NaCl and $MgCl_2$, were 81 and 40 mass %, respectively. It is important to note that the calculated values represent only approximated values as the amorphous phase fractions cannot be determined precisely using this method. SEM images of the combustion synthesized Y-α/β-SiAlON powders are shown in Fig. 3. The α-SiAlON grains obtained using NaCl exhibited equiaxed morphology, although some agglomeration was detected, as is

typical of such synthesis. In contrast, for $MgCl_2$, the powder consisted of mainly rod-like grains, considered to be those of β-SiAlON. The diverse morphologies observed in these products are attributed to the different initial α/β-SiAlON ratios.

Fig. 4 shows the typical temperature profiles during CS of Y-α/β-SiAlON, with the addition of either 12 mass % NaCl or 18 mass % $MgCl_2$. The temperature rapidly reached the maximum value after the reaction was triggered. This was due to large amounts of heat release from the nitridation of Al and Si. The maximum measured temperature was higher in the case of NaCl addition (1912 °C) as opposed to $MgCl_2$ addition (1792 °C), even though a slower heating rate was observed for the former. Due to the increased heating rate in the presence of $MgCl_2$, the production of α-Si_3N_4 was extremely quick, which reduced the time for the formation of α-SiAlON. The overabundant α-Si_3N_4 was thus found to transform into β-Si_3N_4 or β-SiAlON, leading to an increase in the amount of β-phase SiAlON in the final product [14]. Moreover, the formation of β-SiAlON releases less energy compared to α-SiAlON [15]; correspondingly, the overall energy released from the exothermic reaction was lower, and exhibited a lower combustion temperature.

Fig. 5 shows the XRD patterns of the combustion synthesized Ca-α/β-SiAlON, obtained with different salt additives. For the complete nitridation of Si, the same amounts of NaCl (12 mass %) and $MgCl_2$ (18 mass %) were used. Correspondingly, the product obtained with the addition of NaCl exhibited a higher content of α-phase SiAlON (95 %) than $MgCl_2$ (20 %). The corresponding morphologies of the products are shown in Fig. 6. These were analogous to what was observed for the Y-α/β-SiAlON, with the products exhibiting either equiaxed grains of α-SiAlON (for NaCl) or

rod-like and hexagonal β-SiAlON grains (for $MgCl_2$).

Fig. 7 provides the XRD patterns of the combustion synthesized $Y_{0.4}$-α-SiAlON powders obtained using different amounts of NaCl (mass %). The Si peaks weakened as NaCl was increased; nevertheless, Si peaks were detected even at 28 mass % NaCl. However, for more than 28 mass% of NaCl, the combustion reaction could not be completed, which indicated the difficulty in achieving nitridation of Si for the synthesis of $Y_{0.4}$-α-SiAlON.

Fig. 8 shows the XRD patterns of the combustion synthesized $Ca_{0.5}$-α-SiAlON powders obtained using different amounts of NaCl (in mass %). From these patterns, it is noticeable that residual Si and traces of β-SiAlON existed in all the products. No apparent differences in the XRD spectra and SEM images are observed when $CaCO_3$ was used instead of CaO (see Figs. 10 (a) and (b)), although the decomposition of $CaCO_3$ into CaO and CO_2 is expected to absorb a small amount of reaction heat. The XRD patterns of $Ca_{0.5}$-α-SiAlON products combustion synthesized with $MgCl_2$ (in mass %), using $CaCO_3$ as the Ca-source, are displayed in Fig. 9. Here, the phases detected were α- and β-SiAlON, along with residual Si. Compared with Fig. 8, the results demonstrate that the addition of $MgCl_2$ increases the ratio of β-phase SiAlON in the final product; the corresponding rod-like β-SiAlON particles from this reaction are shown in Fig. 10 (c). Several reports have hypothesized that the stability of α-SiAlON can be precisely determined by the presence of oxygen, which leads to an increased amount of β-SiAlON [4]. In this work, the addition of $MgCl_2$ to the starting materials may have promoted the increase of oxygen content during pre-treatment milling, as this salt is highly water-absorbent over NaCl.

Based on these results, we concluded that achieving complete nitridation of Si in the presence of these salts for both Y- and Ca-α-SiAlON is difficult. According to the α-SiAlON formula ($M_xSi_{12-(m+n)}Al_{m+n}O_nN_{16-n}$), as *m* and *n* increase, the amount of the liquid phase M–Si–Al–O, which can form before nitridation of Si, also increases, thus inhibiting the infiltration of N_2. Furthermore, the amount of chloride salt added also increased as *m* and *n* increases owing to the high reaction temperature [24]. As a consequence of the increase in *m* and *n*, nitridation of Si was greatly hindered, and Si remained in the product as an impurity.

The formation mechanism of α-SiAlON from Si, Al, SiO_2, Si_3N_4, AlN, and metal oxides (M_xO_y) has been studied extensively [13,14]. At the early stage of the reaction, Al first reacts with nitrogen gas to form AlN, and the heat released from this reaction enhances the temperature of the sample. The increased temperature leads to the formation of a liquid phase, M–Si–Al–O. As the temperature rises close to the melting point of Si (1410 °C), Si nitridation occurs, eliciting the formation α-Si_3N_4. α-SiAlON is then precipitated from the liquid M–Si–Al–O–N mixture, formed from the dissolution of AlN and Si_3N_4 in the M–Si–Al–O system. When NaCl is used as an inert diluent, the reaction heat is reduced through the latent heat of phase transformation of NaCl. At the preheating zone, NaCl absorbs a portion of the reaction heat through the conversion reaction NaCl (solid) → NaCl (liquid) (ΔH = 82.1 kJ), and thereby reduces the excessive heat released from the reaction Al + 0.5N_2 (g) → AlN (ΔH = −318.0 kJ). Consequently, the melting and agglomeration of the Si particles in the starting materials are greatly reduced, and the infiltration of N_2 is enhanced. Then, as the reaction, 3Si + 2N_2 (g) →α-Si_3N_4 (ΔH = −828.9 kJ), proceeds, α-Si_3N_4 is generated,

initiating the release of a large amount of heat. AlN and α-Si_3N_4 begin to dissolve in the liquid M–Si–Al–O, and hence a new liquid phase, M–Si–Al–O–N system is formed. Precipitation of α-SiAlON occurs simultaneously with the formation of this system. At this stage, NaCl absorbs a large amount of heat through the reaction, NaCl (liquid) → NaCl (gas) (ΔH = +202.1 kJ), and then separates out of the reaction system.

To summarize, the salt additives can be considered heat sinks given that they absorb and remove the excessive heat released upon nitridation of Al and Si in the form latent heat of melting and evaporation, respectively; this assumption ignores other small endo-/exothermic reactions such as Al and Si melting. The reduced heat provides for steady combustion wave propagation, thus improving the conversion rate. The basis for using varying amounts of NaCl and $MgCl_2$ for total nitridation is the different endothermicity of each chloride, which has been detailed in our previous work [19]. The more rapid heating rate with $MgCl_2$ as the diluent can be rationalized as follows: within the combustion front, the salt melts by absorbing the reaction heat to form a wet $MgCl_2$–AlN–M_xO_y system surrounding the Si particles through capillary forces. Raising the amount of melted $MgCl_2$ increases the probability of particle–particle contact, and hence, accelerates the Si_3N_4–AlN–M_xO_y diffusion reaction that results in SiAlON nuclei formation, prompting a relatively higher heating rate as opposed to when NaCl is used.

The results in this work indicate NaCl or $MgCl_2$ are potential additives for large-scale production of SiAlON powders. Note that the production efficiency can be greatly improved because of the small amount of additive (12 and 18 mass % for NaCl and $MgCl_2$, respectively)

based on latent heat and sensible heat, compared with the addition of Si_3N_4 (approximately 45 mass %) based on only sensible heat. Furthermore, the cost of post-synthesis treatments such as milling will be decreased by adding these salts, which effectively prevented the products from self-sintering. Moreover, the α/β-SiAlON ratio and morphology of the products can be controlled by changing metal chloride content. Therefore, the overall production cost of SiAlON can be significantly reduced. The lower price and the designed phase of these products may open up new applications for these materials.

4. Conclusions

High purity Y- and Ca-α/β-SiAlON composite ceramics and α-SiAlON were successfully synthesized by using a salt-assisted combustion method under 1 MPa N_2 pressure. The latent heat of the salts permitted the absorption of the heat released from the starting materials, thereby promoting the complete nitridation of Si. The α/β-SiAlON ratio and morphology of the products were strongly affected by the type of chloride employed: in the presence of NaCl, the amount of α-phase increased, while the amount of β-phase SiAlON increased when $MgCl_2$ was used. Notably, the morphology of the product changed corresponding to the α/β-SiAlON ratio, equiaxed to rod-like grains as the α/β ratio decreased. These findings demonstrate a novel and facile approach for fabricating high-quality α/β-SiAlON ceramics or α-SiAlON via a salt-assisted combustion method.

Acknowledgements

This work was financially supported by the 2013 Strategic Foundational Technology Improvement Support Operation, Ministry of Economy, Trade and Industry (No. 24110105008, Development of high-quality and economical SiAlON powders by combustion synthesis method).

References

[1] K.H. Jack, Review Sialons and related nitrogen ceramics, J. Mater. Sci. 11 (1976) 1135-1158.

[2] T. Ekström, P.O. Käll, M. Nygren, P.O. Olssen, Dense single-phase β-sialon ceramics by glass-encapsulated hot isostatic pressing, J. Mater. Sci. 24 (1989) 1853-1861.

[3] T. Ekström, M. Nygren, SiAlON Ceramics, J. Am. Ceram. Soc. 75[2] (1992) 259-276.

[4] S. Bandyopadhyay, M.J. Hoffmann, G. Petzow, Densification Behavior and Properties of Y_2O_3-Containing α-SiAlON-Based Composites, J. Am. Ceram. Soc. 79 (1996) 1537-1545.

[5] T.-S. Sheu, Microstructure and Mechanical Properties of the in situ β-Si_3N_4/α′-SiAlON Composite, J. Am. Ceram. Soc. 77 (1994) 2345-2353.

[6] F. Ye, L. Liu, H. Zhang, Y. Zhou, Z. Zhang, Novel mixed α/β-SiAlONs with both elongated α and β grains, Scripta Mater. 60 (2009) 471-474.

[7] Y.-W. Li, P.-L. Wang, W.-W. Chen, Y.-B. Cheng, D.-S. Yan, Phase formation and microstructural evolution of Ca α-sialon using different Si_3N_4 starting powders, J. Eur. Ceram. Soc. 20 (2000) 1803-1808.

[8] J.W.T. van Rutten, H.T. Hintzen, R. Metselaar, Phase formation of Ca-α-sialon by reaction sintering, J. Eur. Ceram. Soc. 16 (1996) 995-999.

[9] J. Huang, H. Zhou, Z. Huang, G. Liu, M. Fang, Y.g. Liu, Preparation and Formation Mechanism of Elongated (Ca,Dy)-α-Sialon Powder via Carbothermal Reduction and Nitridation. J. Am. Ceram. Soc. 95 (2012) 1871-1877.

[10] K. Aoyagi, T. Hiraki, R. Sivakumar, T. Watanabe, T. Akiyama, A new route to synthesize

β-$Si_{6-z}Al_zO_zN_{8-z}$ powders, J. Alloys. Compd 441 (2007) 236-240.

[11] K. Aoyagi, T. Hiraki, R. Sivakumar, T. Watanabe, T. Akiyama, Mechanically Activated Combustion Synthesis of β-$Si_{6-z}Al_zO_zN_{8-z}$ (z=1–4), J. Am. Ceram. Soc. 90 (2007) 626-628.

[12] X. Yi, K. Watanabe, T. Akiyama, Fabrication of dense [beta]-SiAlON by a combination of combustion synthesis (CS) and spark plasma sintering (SPS), Intermetallics 18 (2010) 536-541.

[13] G. Liu, C. Pereira, K. Chen, H. Zhou, X. Ning, J.M.F. Ferreira, Fabrication of one-dimensional rod-like α-SiAlON powders in large scales by combustion synthesis, J. Alloys. Compd 454 (2008) 476-482.

[14] G. Liu, K. Chen, H. Zhou, X. Ning, C. Pereira, J.M.F. Ferreira, Fabrication of yttrium-stabilized α-SiAlON powders with rod-like crystals by combustion synthesis, J. Mater. Sci. 41 (2006) 6062-6068.

[15] C.L. Yeh, F.S. Wu, Y.L. Chen, Effects of alpha- and beta-Si_3N_4 as precursors on combustion synthesis of (alpha plus beta)-SiAlON composites, J. Alloys. Compd. 509 (2011) 3985-3990.

[16] C.L. Yeh, K.C. Sheng, Effects of alpha-Si_3N_4 and AlN addition on formation of alpha-SiAlON by combustion synthesis, J. Alloys. Compd 509 (2011) 529-534.

[17] G. Liu, K. Chen, H. Zhou, X. Ning, J.M.F. Ferreira, Effect of diluents and NH_4F additive on the combustion synthesis of Yb α-SiAlON, J. Eur. Ceram. Soc. 25 (2005) 3361-3366.

[18] J. Niu, X. Yi, I. Nakatsugawa, T. Akiyama, Salt-assisted combustion synthesis of β-SiAlON

fine powders, Intermetallics 35 (2013) 53-59.

[19] J. Niu, K. Harada, I. Nakatsugawa, T. Akiyama, Morphology control of β-SiAlON via salt-assisted combustion synthesis, Ceram. Inter. 40 (2014) 1815-1820.

[20] G.Z. Cao, R. Metselaar, .alpha.'-Sialon ceramics: a review, Chem. Mater. 3 (1991) 242-252.

[21] C.L. Hewett, Y.-B. Cheng, B.C. Muddle, M.B. Trigg, Phase Relationships and Related Microstructural Observations in the Ca-Si-Al-O-N System, J. Am. Ceram. Soc. 81 (1998) 1781-1788.

[22] C. P.Gazzara, D.R. Messier, Determination of phase content of Si_3N_4 by X-Ray diffraction analysis, Ceram. Bull. 56 (1977) 777-780.

[23] H.I. Won, C.W. Won, H.H. Nersisyan, K.S. Yoon, Salt-assisted combustion synthesis of silicon nitride with high [alpha]-phase content, J. Alloys. Compd 496 (2010) 656-659.

[24] S. Bandyopadhyay, G. Petzow, Formation of multiphase SiAlON ceramic, Mater. Chem. Phys. 61 (1999) 9-13.

Figure captions

Fig. 1 XRD patterns of combustion synthesized Y-α/β-SiAlON with the addition of varied amounts of NaCl (mass %), for which powders of Si, Al, Y_2O_3, and NaCl were mixed and a single end ignited.

Fig. 2 XRD patterns of combustion synthesized Y-α/β-SiAlON powders obtained using optimized amounts of (a) NaCl (12 mass %) and (b) $MgCl_2$ (18 mass %). The ratio of α-phase SiAlON is 81 mass % in sample (a) and is 40 mass % in sample (b).

Fig. 3 SEM images of combustion synthesized Y-α/β-SiAlON powders using (a) NaCl (12 mass %) and (b) $MgCl_2$ (18 mass %), in which rod-like products are β-SiAlON. Scale bars provided.

Fig. 4 Typical temperature profiles recorded during combustion synthesis of Y-α/β-SiAlON with the addition of (a) NaCl (12 mass %) and (b) $MgCl_2$ (18 mass %), illustrating the dependence on the type and amount of chloride used. (inset) Schematic of the combustion synthesis chamber employed for this study.

Fig. 5 XRD patterns of combustion synthesized Ca-α/β-SiAlON powders, obtained using optimized amounts of (a) NaCl (12 mass %) and (b) $MgCl_2$ (18 mass %), for which powders of Si, Al, CaO were mixed with NaCl or $MgCl_2$ and ignited. Major component of the product was either (a) α- or (b) β-SiAlON.

Fig. 6 SEM images of synthesized Ca-α/β-SiAlON powders using (a) NaCl (12 mass %) and (b) $MgCl_2$ (18 mass %). Product (a) displays fewer rod-like SiAlON while an increase in density is observed in product (b). Scale bars provided as insets.

Fig.7 XRD patterns of combustion synthesized $Y_{0.4}$-α-SiAlON powders using different amounts of NaCl (mass %). Note that all products consist of α-SiAlON and unreacted silicon. No peaks corresponding to the β-equivalent are observed.

Fig.8 XRD patterns of the combustion synthesized $Ca_{0.5}$-α-SiAlON powders obtained using different amounts of NaCl (mass %). With $CaCO_3$ or CaO as the initial Ca-source, no significant differences are observed. All products consist of α-SiAlON with some unreacted silicon.

Fig. 9 XRD patterns of combustion synthesized $Ca_{0.5}$-α-SiAlON powders obtained with the addition of different amounts of $MgCl_2$ (mass %) using $CaCO_3$ as the Ca source. The major component of the product was β-SiAlON with some unreacted silicon.

Fig. 10 SEM images of the synthesized $Ca_{0.5}$-α-SiAlON powders using 30 mass % of various salt additives: (a) NaCl, $CaCO_3$, (b) NaCl, CaO, and (c) $MgCl_2$, $CaCO_3$. Note that products (a) & (b) areα-SiAlON , but the product (c) exhibits large rod-likeβ-equivalents. $CaCO_3$ and CaO are the Ca sources in each case. Scale bars provided as insets.

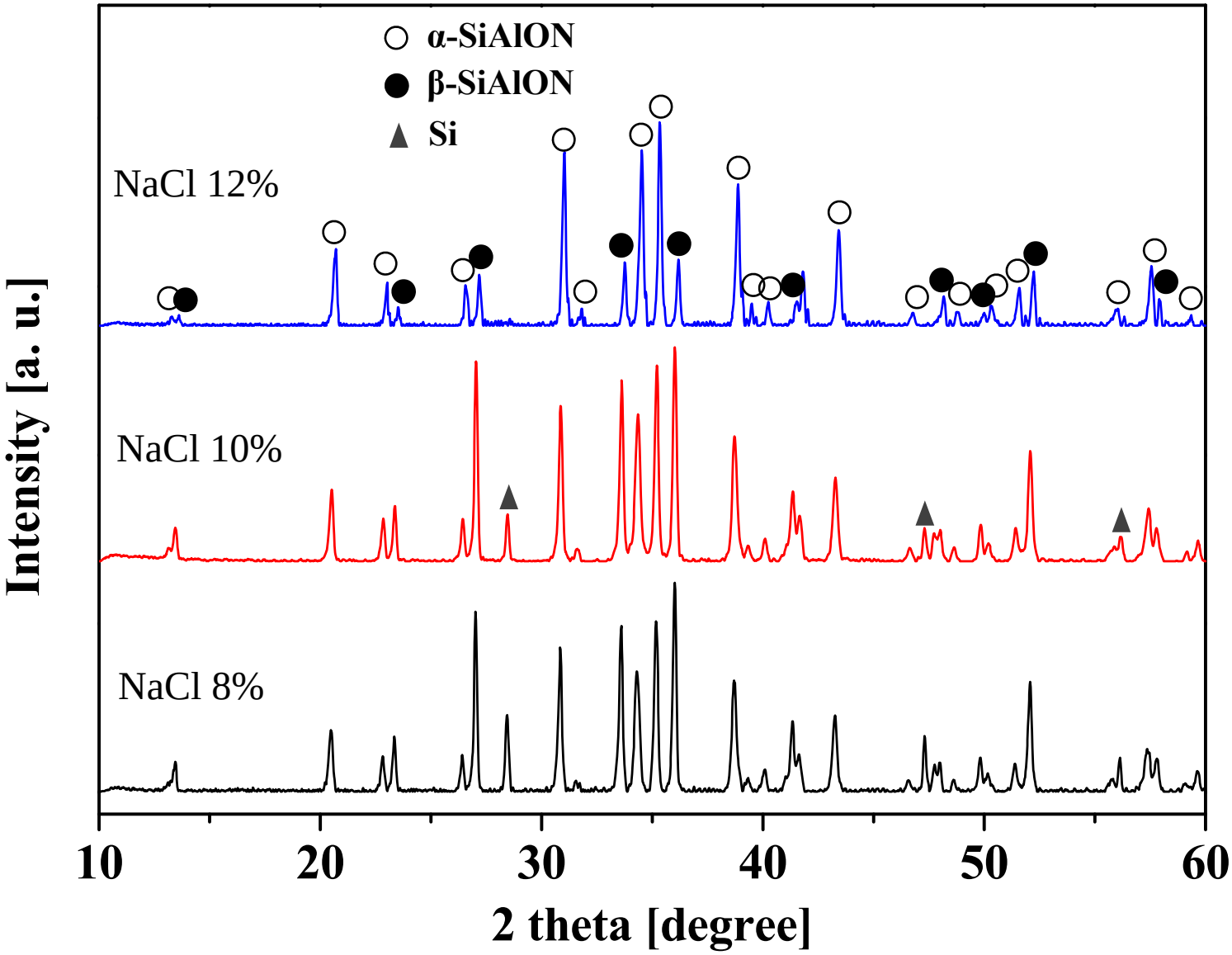
α-SiAlON
β-SiAlON
Si
NaCl 12%
NaCl 10%
NaCl 8%
Intensity [a. u.]
10
20
30
40
50
60
2 theta [degree]

Fig. 1

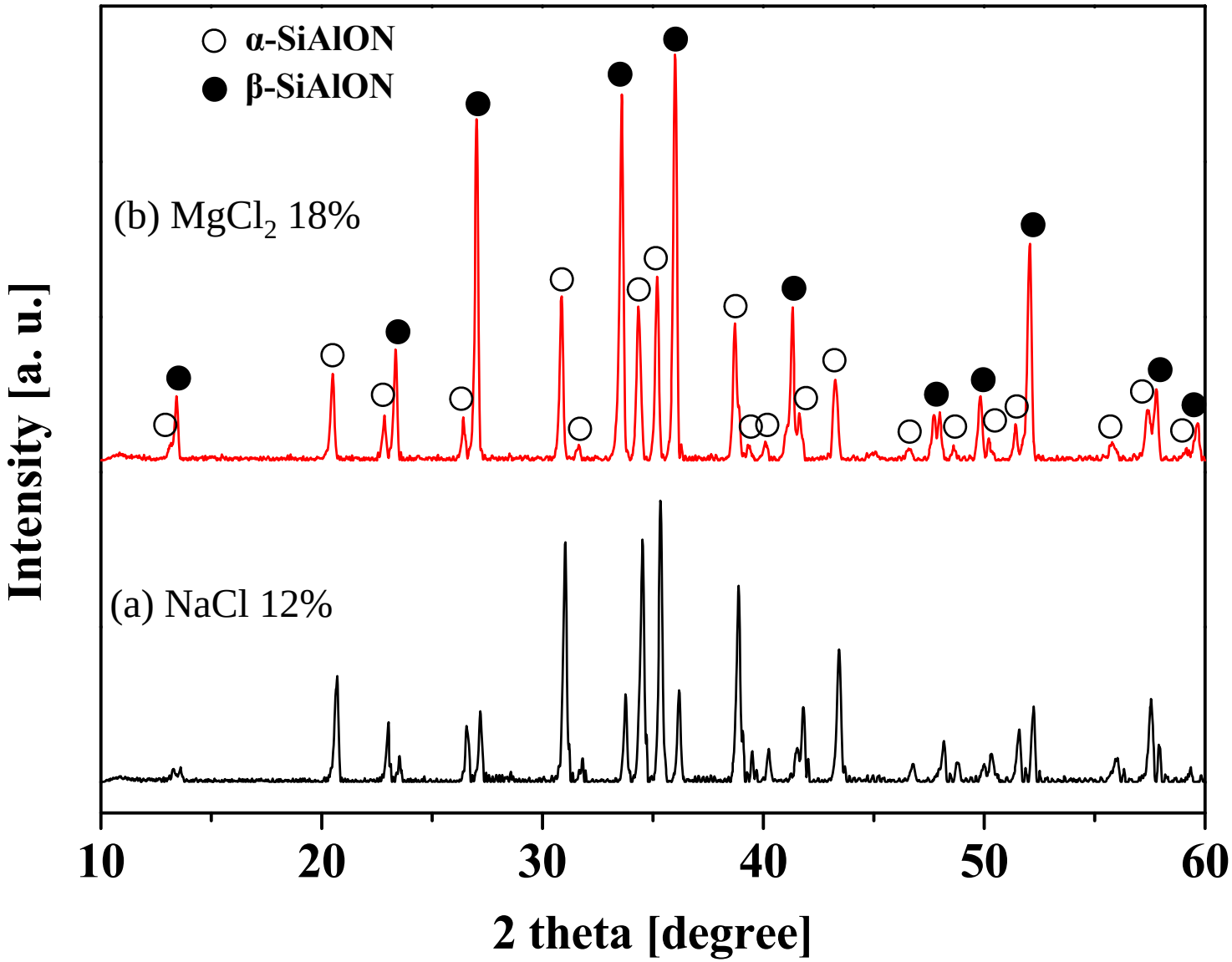
α-SiAlON
β-SiAlON
(b) MgCl2 18%
(a) NaCl 12%
Intensity [a. u.]
10
20
30
40
50
60
2 theta [degree]

Fig. 2

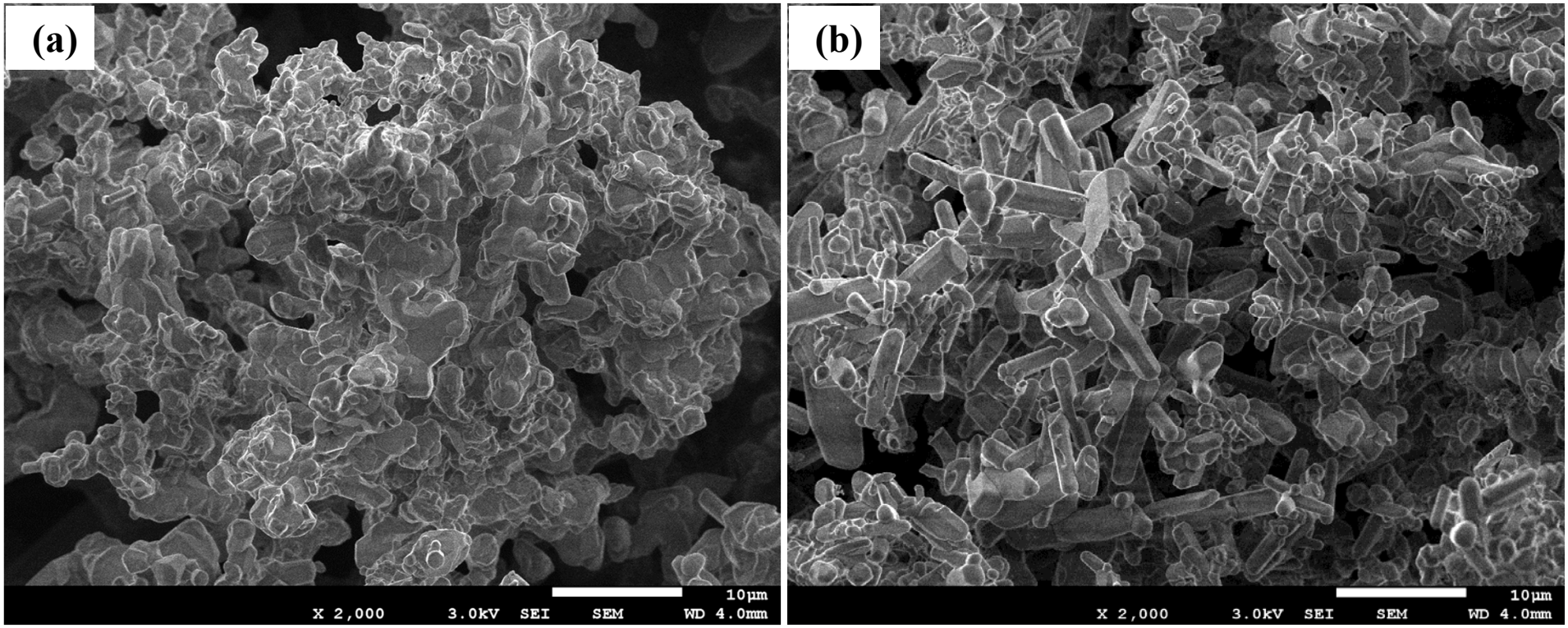
(a)
10μm
X 2,000 3.0kV SEI SEM WD 4.0mm
(b)
10μm
X 2,000 3.0kV SEI SEM WD 4.0mm

Fig. 3

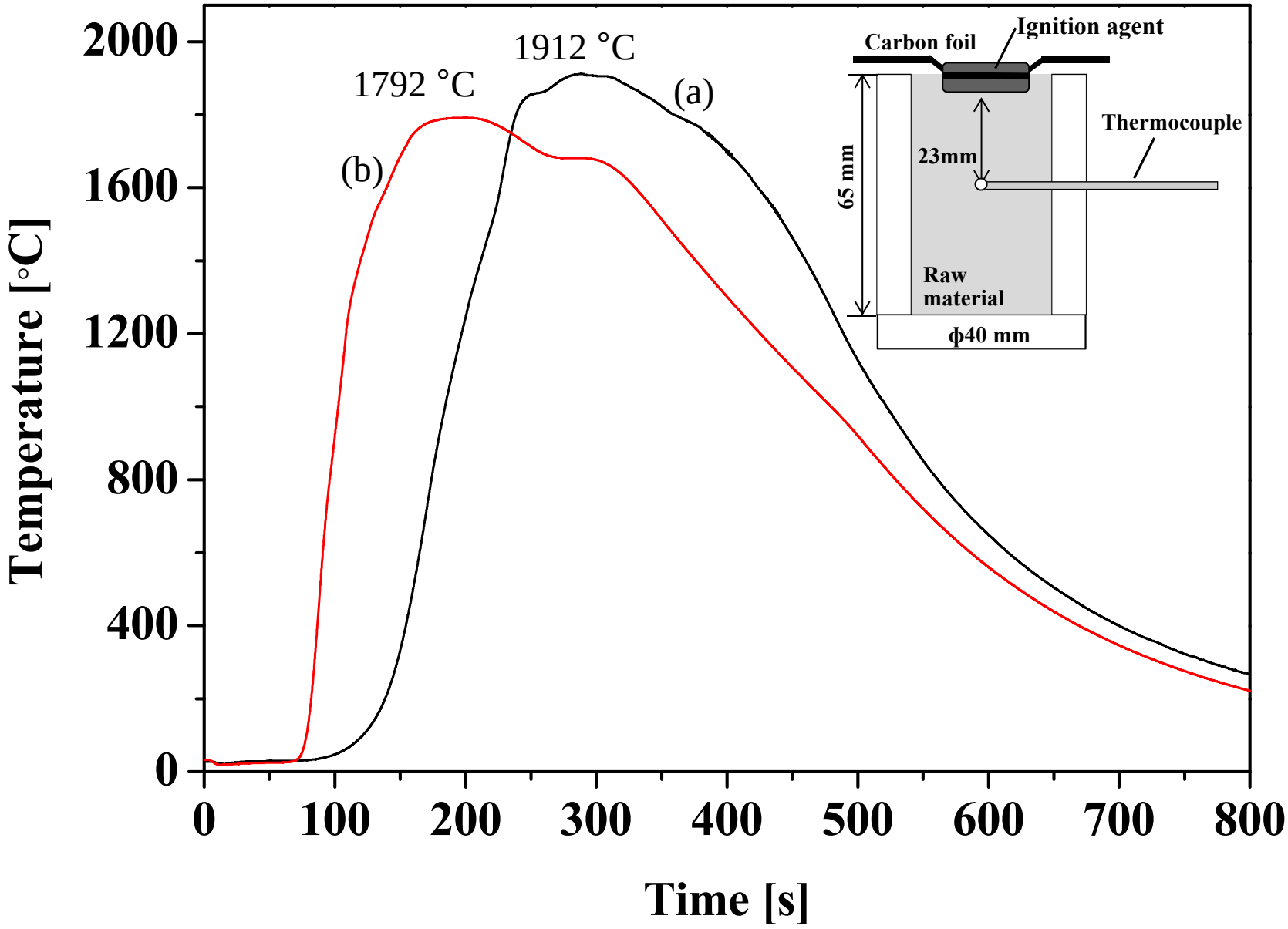
2000
1600
1200
800
400
0
Temperature [°C]
0
100
200
300
400
500
600
700
800
Time [s]
1912 °C
1792 °C
(a)
(b)
Carbon foil
Ignition agent
Thermocouple
23mm
65 mm
Raw material
ϕ40 mm

Fig. 4

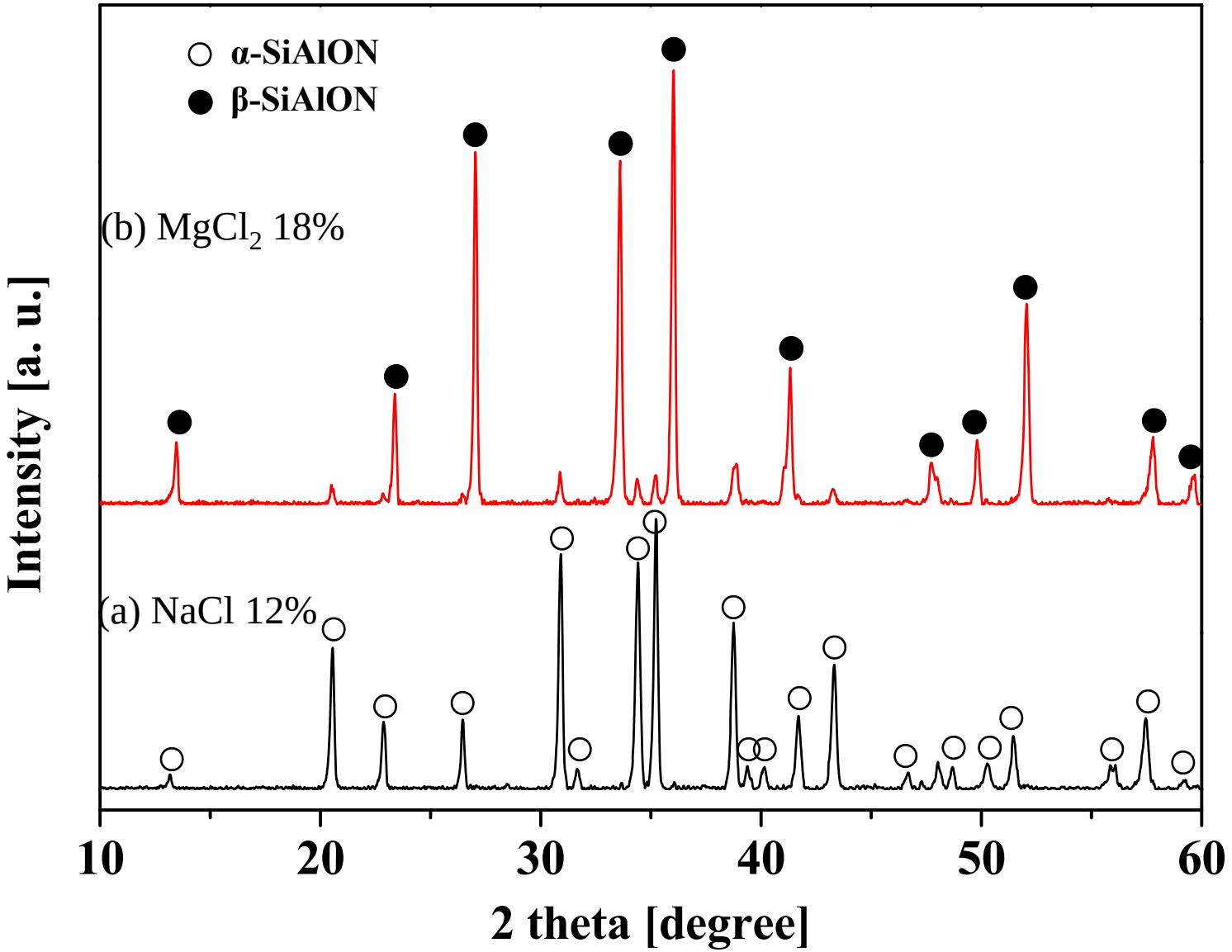
α-SiAlON
β-SiAlON
(b) MgCl2 18%
(a) NaCl 12%
Intensity [a. u.]
10
20
30
40
50
60
2 theta [degree]

Fig. 5

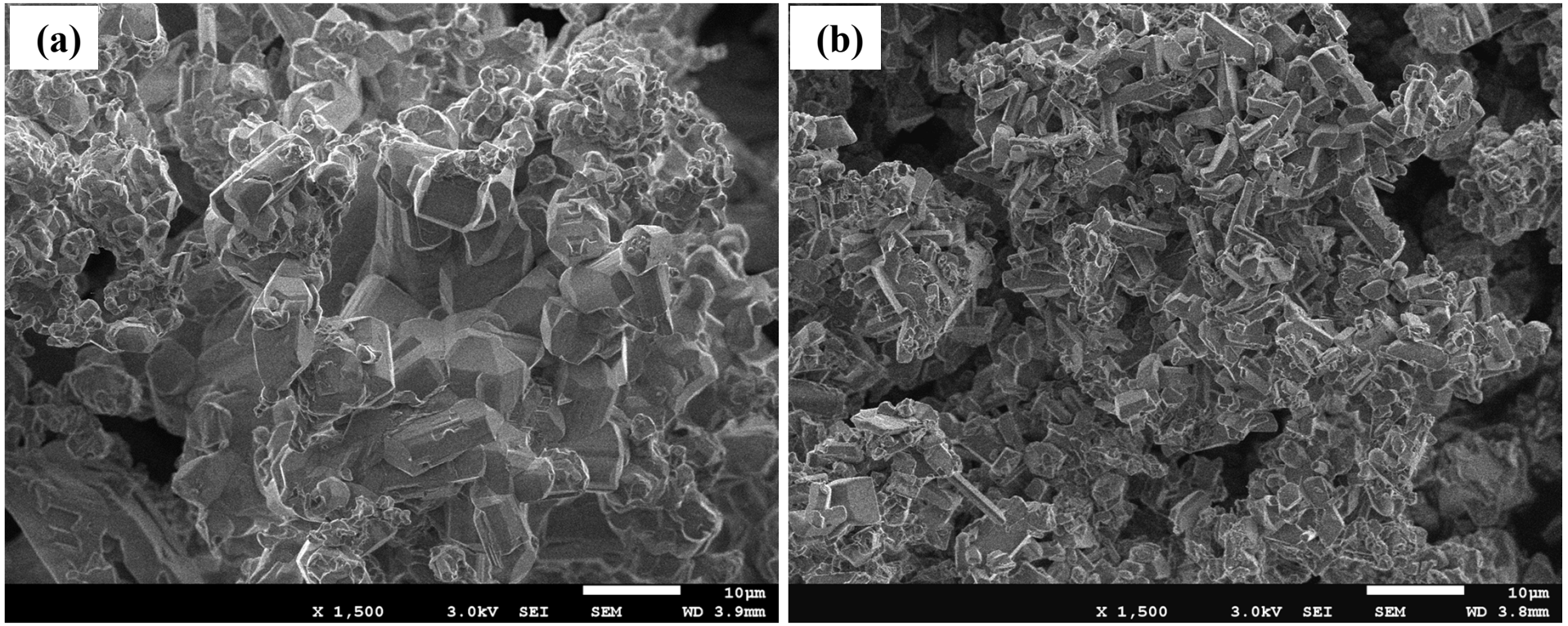
(a)
10µm
X 1,500 3.0kV SEI SEM WD 3.9mm
(b)
10µm
X 1,500 3.0kV SEI SEM WD 3.8mm

Fig. 6

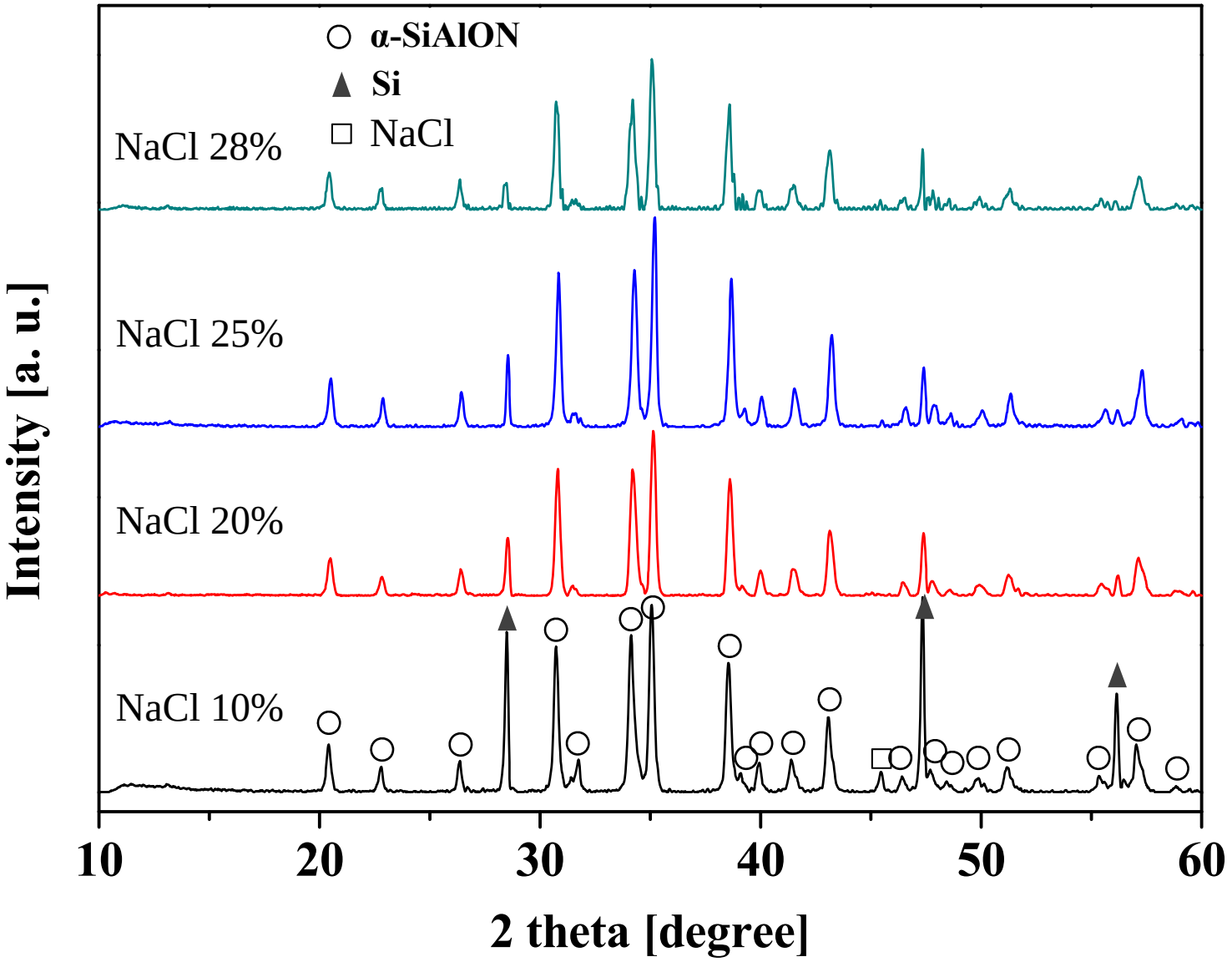
α-SiAlON
Si
NaCl
NaCl 28%
NaCl 25%
NaCl 20%
NaCl 10%
Intensity [a. u.]
10
20
30
40
50
60
2 theta [degree]

Fig. 7

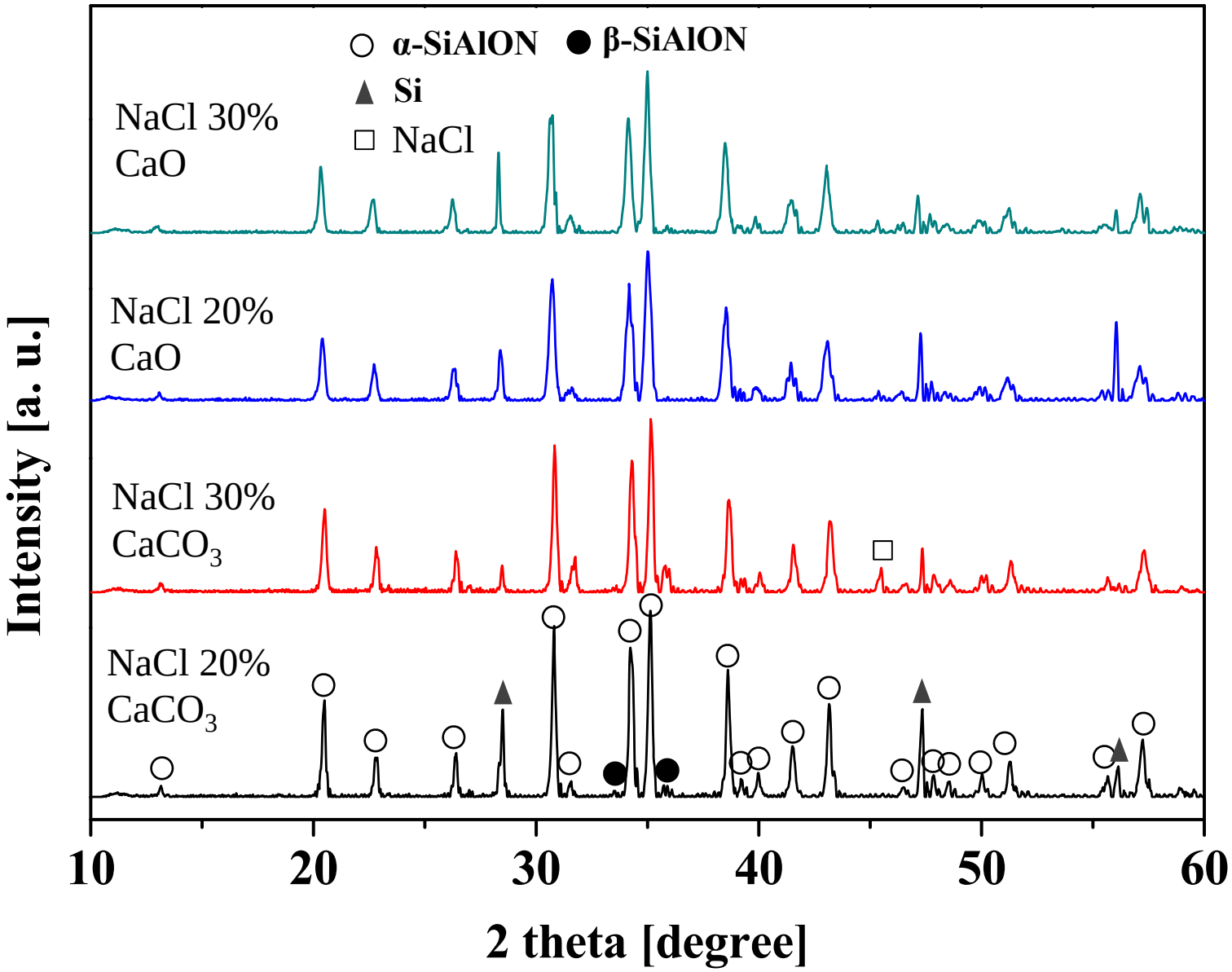
○ α-SiAlON ● β-SiAlON
▲ Si
□ NaCl
NaCl 30%
CaO
NaCl 20%
CaO
NaCl 30%
CaCO3
NaCl 20%
CaCO3
Intensity [a. u.]
10
20
30
40
50
60
2 theta [degree]

Fig. 8

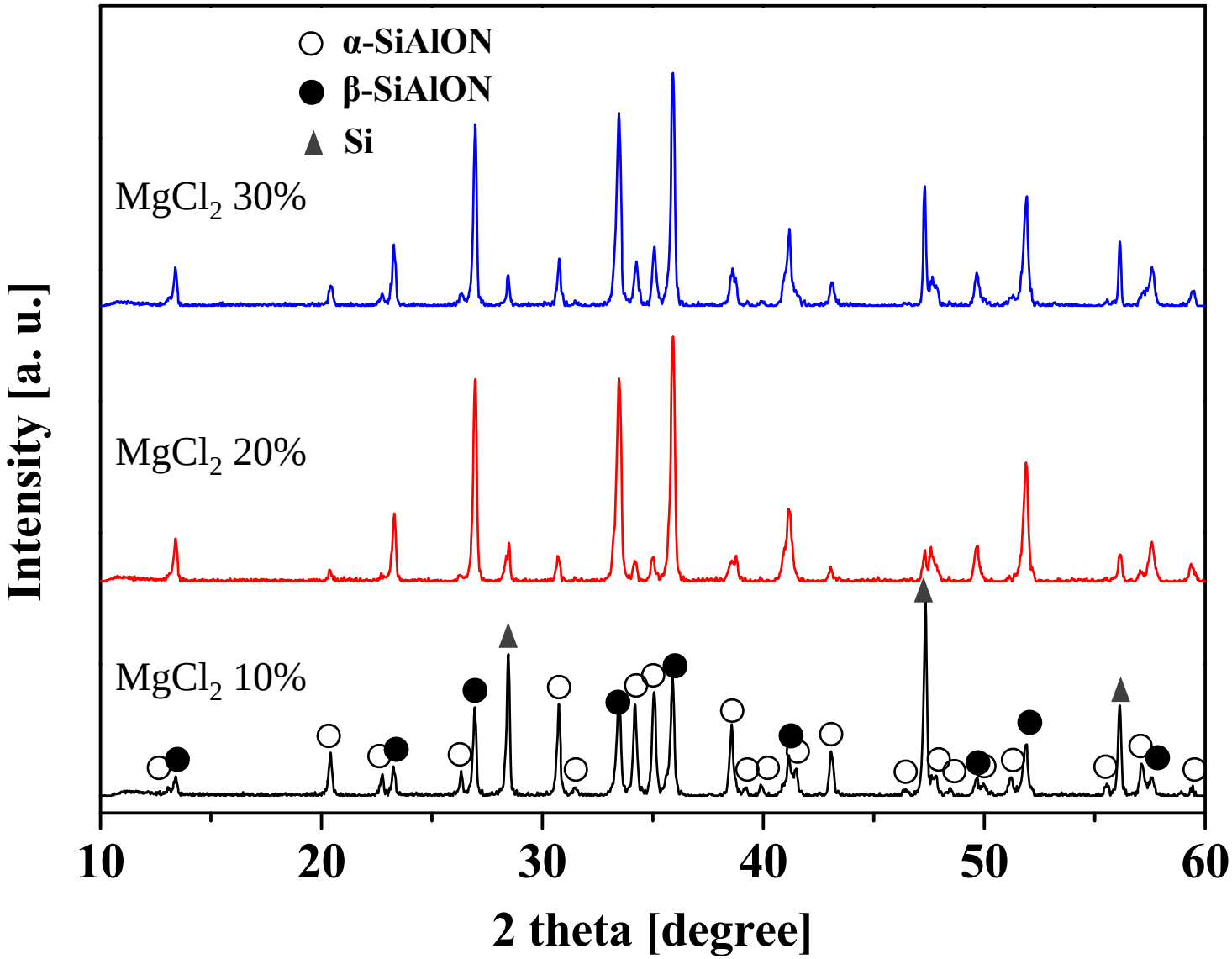
α-SiAlON
β-SiAlON
Si
MgCl2 30%
MgCl2 20%
MgCl2 10%
Intensity [a. u.]
10
20
30
40
50
60
2 theta [degree]

Fig. 9

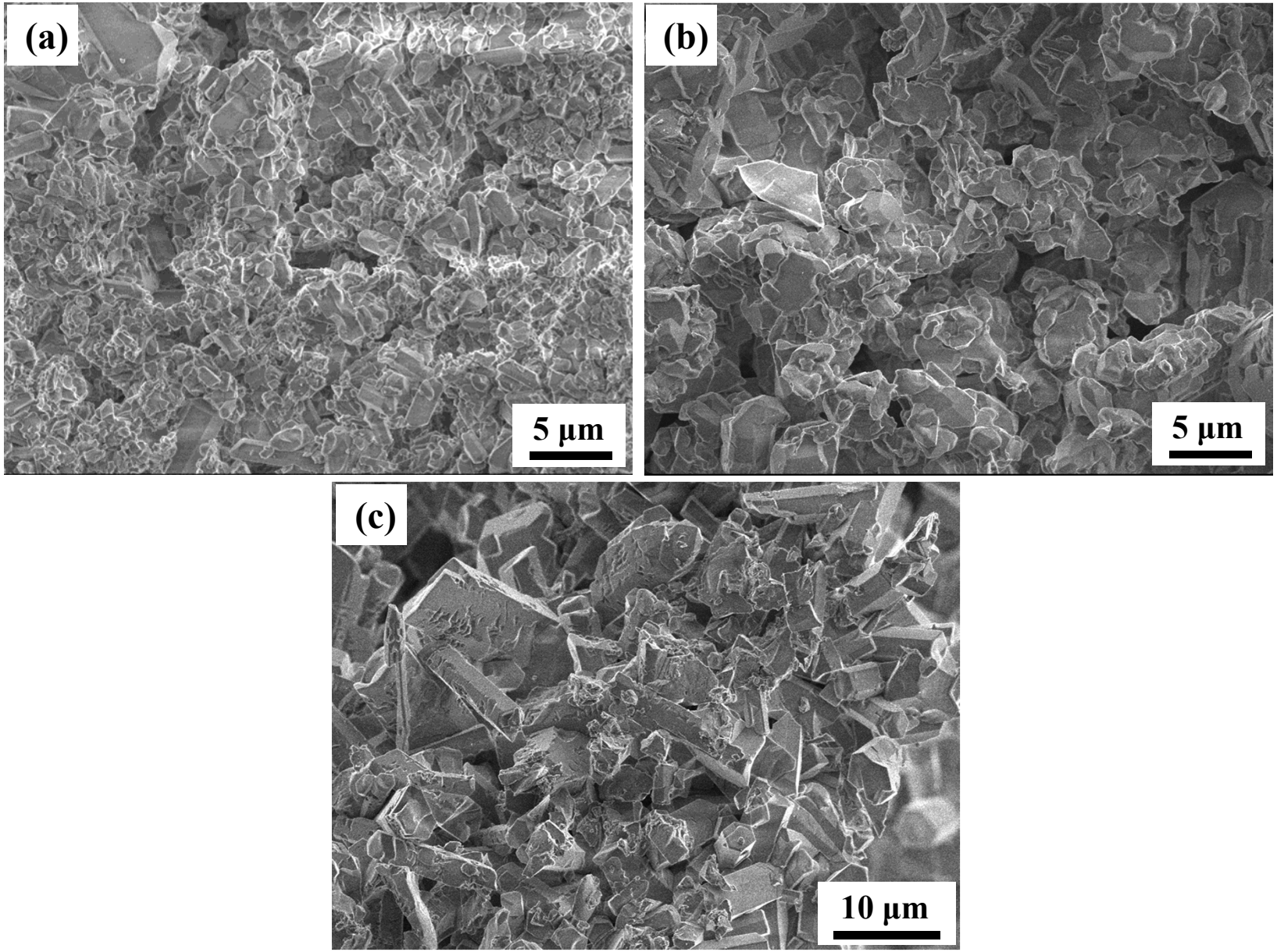

Fig. 10